ELSEVIER

Dyes and Pigments, Vol. 38, No. 4, pp. 227–242, 1998

Printed in Great Britain
PII: S0143-7208(98)00003-5 0143-7208/98 $19.00+0.00

Color Change on Deprotonation of 5-(8,8-dicyanoheptafulven-3-yl)-2-hydroxy-1,3-xylyl-18-crown-5

K. Yumura[a], H. Otani[a] & J. Mizuguchi[b]*

[a]Department of Chemistry, Faculty of Education, Yokohama National University 79-5 Tokiwadai, Hodogaya-ku, 240-8501 Yokohama, Japan
[b]Department of Applied Physics, Faculty of Engineering, Yokohama National University 79-2 Tokiwadai, Hodogaya-ku, 240-8501 Yokohama, Japan

(Received 24 November 1997; accepted 5 January 1998)

ABSTRACT

Compound 5-(8,8-dicyanoheptafulven-3-yl)-2-hydroxy-1,3-xylyl-18-crown-5 is a novel non-benzenoid crown ether dye derived from 8,8-dicyanoheptafulvene together with a crown ether having a phenolic hydroxide group in its cavity. The color change on deprotonation has been UV/Vis-spectroscopically investigated with special attention to the metal-selective coloration, using a variety of alkali metal bases. Deprotonation brought about a significant color change from red to blue ($\lambda_{max} \approx 430 \rightarrow 640$ nm), but quite irrespective of the cation species of the base added. In addition, the coloration is found to be very similar to that of the uncrowned 8,8-dicyanoheptafulvene-substituted phenol. Interestingly, geometry optimization by MO calculations revealed that the crown ether ring is heavily deformed due to lone pair repulsion of the oxygen atoms in the cavity, making the hydroxide group directly exposed to the surrounding environment. Thus, the electronic state of the title compound is almost equivalent to that of the uncrowned compound. This explains why no cation-dependent coloration takes place and why the bathochromic displacement is mainly due to π-electron delocalization of the phenoxide ($-O^-$) into the heptafulvene chromophore.

Keywords: Deprotonation, chromophore, crowned dye, electronic spectra, MO calculations.

*Corresponding author.

INTRODUCTION

Stable, non-benzenoid compounds, characterized by large permanent dipole moments, are frequently colored in spite of their small molecular weights. For example, non-benzenoid azulene has a brilliant blue color; whereas naphthalene, an isomer of azulene, is colorless [1]. We regard this kind of non-benzenoid systems as a potential chromophore and focus our attention on 8,8-dicyanoheptafulvene. In previous work [2], we synthesized 8,8-dicyano-3-(4′-hydroxy)phenyl-heptafulvene (designated as uncrowned heptafulvene phenol **1a** in Fig. 1) and studied its spectral and conformational

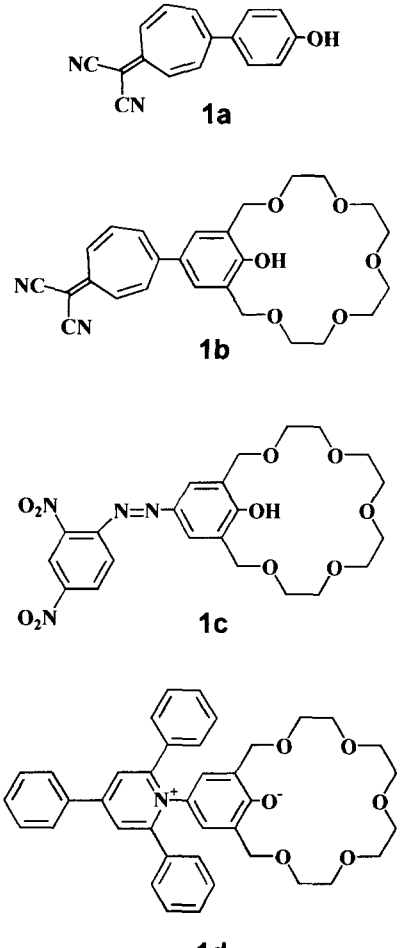

Fig. 1. Conformation of uncrowned and crowned ether dyes: uncrowned heptafulvene phenol (**1a**) [2], crowned 4-(8,8-dicyanoheptafulven-3-yl)phenol (**1b**), crowned 2,4-dinitrophenyl-azophenol (**1c**) [3][4] and crowned pyridinium *N*-phenoxide betaine (**1d**) [5].

changes on deprotonation. Deprotonation at the hydroxy moiety induces a large spectral shift due to electron delocalization from the phenoxide ($-O^-$) ion into the whole chromophore, accompanied by enhanced conjugation (reduction in torsion angle) between the seven-membered ring and the phenyl ring. These results are also supported by ^{13}C NMR chemical shifts and molecular orbital (MO) calculations.

In the present investigation, we have synthesized 5-(8,8-dicyano heptafulven-3-yl)-2-hydroxy-1,3-xylyl-18-crown-5 (compound **1b** in Fig. 1) by extending the 8,8-dicyanoheptafulvene moiety with 2-hydroxy-1,3-xylyl-18-crown-5 having a phenolic hydroxide group in its cavity. Crowned dye such as crowned 2,4-dinitrophenyl azophenol **1c** [3,4] as well as crowned pyridinium *N*-phenoxide betaine **1d** [5] are already known (Fig. 1). For these compounds, the metal-selective coloration is interpreted in the manner that the metal cation included in the cavity of the crown ether induces an electrostatic influence on the phenoxide moiety, giving rise to a variety of colors [6] (Fig. 2). The same coloration mechanism can be expected for compound **1b**, as judged from its structure.

The present investigation aims at clarifying the mechanism of the metal-selective coloration on deprotonation with various bases: for example, with lithium hydroxide, the cation of which (Li^+: 0.60 Å) is small enough to be included in the cavity, and with tetra-*n*-butylammonium hydroxide (TBAH), which has a cation much larger than the crown ether ring. Attention is especially focused on the quantitative deprotonation reaction, as monitored by the electrical conductivity of the solution ('conductometric titration').

We report also the results of the conformational and UV/Vis spectral changes of compound **1b** on deprotonation and discuss the coloration mechanism on the basis of MO calculations.

EXPERIMENTAL

Chemicals

Commercially available bases MOH (M = Li, Na, K, Rb and Cs and [*n*-butyl]$_4$N), alkali-metal iodides MI (M = Li, Na, K, Rb and Cs) as well as organic solvents [dimethylsulfoxide (DMSO), acetonitrile, ethanol, tetrahydrofuran (THF)] of guaranteed reagent were used without further purification.

Measurements

UV/Vis spectra were recorded on a Shimadzu UV-2400PC spectrophotometer. Electrical conductivity in solution was measured with an Iuchi Cyber Scan conductometer (Model CON100).

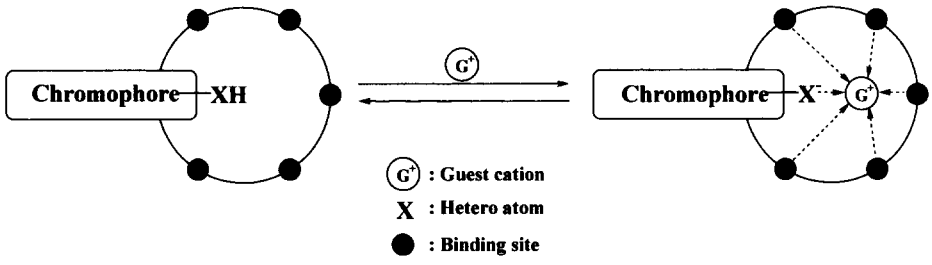

Fig. 2. Schematic representation of the deprotonation reaction in crown ether dyes and its cation-dependent coloration mechanism (E2 type) [6].

Deprotonation experiments were carried out by adding 10 μl of a 0.1 M base to a solution of compound **1b** in each solvent (*ca* 4.5×10^{-4} M; 50 ml) under argon (degassed), while monitoring the absorption spectra as well as the electrical conductivity of the solution ('conductometric titration'). The same procedure was also used for the addition of alkali metal iodides to a solution of compound **1b** in DMSO.

MO calculations

Geometry for compound **1b** and its deprotonated species were optimized by means of the AM1 Hamiltonian in MOPAC 6 [7]. The INDO/S program used for spectroscopic calculations is part of the ZINDO program package [8]. Optical absorption bands were computed on the optimized geometry using the INDO/S Hamiltonian. 145 Configurations were considered for the configuration interaction (CI). All calculations were performed on a Power Macintosh 8500/120 computer.

RESULTS AND DISCUSSION

Synthesis

The synthetic procedure for compound **1b** is outlined in Scheme 1. Compound **2a** was initially prepared by a three step reaction, from 4-bromo-2,6-dimethylphenol on the basis of 2-methoxy-1,3-xylyl-18-crown-5 [9]. The bromine atom was then substituted by lithium by means of *tert*-butyllithium to give compound **2b**. Subsequent transmetalation with zinc chloride yielded compound **2c**. Compound **2c** then reacted readily with compound **3**, derived from 8,8-dicyanoheptafulvene [10], in the presence of 20 mol% of Pd(0)-catalyst prepared *in situ* by reduction of bis(triphenylphosphine)palladium

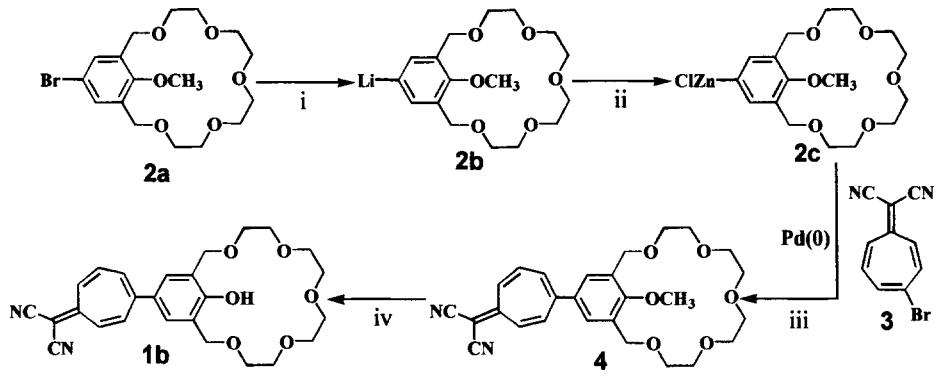

Scheme 1 Reagents and conditions: (i) 2.0eq *tert*-C_4H_9Li/abs. THF, −72°C, 1h; (ii) 1.2eq $ZnCl_2$/abs. THF, −72°C~rt, 2h; (iii) 20 mol% $Cl_2Pd(PPh_3)_2$-DIBAL-H/abs. THF, rt, 1h; (iv) 3.0eq LiI/dry pyridine, reflux, 4h (overall yield based on compound **3**:52%).

dichloride $Cl_2Pd(PPh_3)_2$ with diisobutylaluminium hydride (DIBAL-H) to give compound **4** (yield: 68%) [11]. Finally, compound **1b** was obtained as red needles by demethylating compound **4** with lithium iodide in pyridine (yield: 76%). The overall yield based on compound **3** was 52%.

(2-Methoxy-1,3-xylyl-18-crown-5)-5-zinc chloride **2c**

A solution of 1.7 mol·dm^{-3} of *tert*-butyllithium in pentane (3.0 cm^{-3}, 5.1 mmol) was added dropwise to a solution of 5-bromoanisole **2a** (1.01 g, 2.5 mmol) in dry THF (10 cm^{-3}) at −72°C under argon. After stirring for 1 h at −72°C, to the resulting solution was added a solution of anhydrous zinc chloride (0.41 g, 3.0 mmol) in dry THF (10 cm^{-3}). The mixture was stirred for an additional *ca* 1 h at −72°C and then for *ca* 1 h at room temperature, giving (2-methoxy-1,3-xylyl-18-crown-5)-5-zinc chloride **2c**.

5-(8,8-Dicyanoheptafulven-3-yl)-2-methoxy-1,3-xylyl-18-crown-5 **4**

A solution of Pd(0) catalyst prepared by treating $Cl_2Pd(PPh_3)_2$ (0.28 g, 0.4 mmol) suspended in dry THF (5 cm^{-3}) with 1.5 mol·dm^{-3} of DIBAL-H in toluene (0.5 cm^{-3}, 0.8 mmol) was added to a THF solution of zinc reagent **2c** at room temperature under argon, and was then added a solution of 3-bromo-8,8-dicyanoheptafulvene **3** (0.51 g, 2.0 mmol) in dry THF (10 dm^{-3}). After stirring for 4 h at room temperature, the solution was poured into 3 mol·dm^{-3} cold hydrochloric acid and extracted with ethyl acetate. The extract was washed with saturated aqueous sodium chloride, dried, and evaporated to dryness. Column chromatography on silica gel with ethyl acetate as the eluent yielded 5-(8,8-dicyanoheptafulven-3-yl)-2-methoxy-1,3-xylyl-18-crown-5 **4**, which was recrystallized twice from carbon tetra-

chloride–hexane. Yield 68%. Red needles; mp 157–158°C (Found: M^+, 478.2127, $C_{27}H_{30}N_2O_6$ requires M, 478.2104); ν_{max}/cm^{-1} 2185 (C≡N) ; δ_H ($CDCl_3$) 3.66~3.48 (m, 16H, -OCH_2CH_2O-), 4.19 (s, 3H, -OCH_3), 4.60 (s, 4H, benzylic H), 6.99~7.06 (m, 2H, 4- and 5-H), 7.30~7.35 (m, 2H,1- and 6-H), 7.37 (s, 2H, aromatic H), 7.44 (dd, 1H, 2-H); δ_C ($CDCl_3$) 65.28 (-OCH3), 68.54 (8-C), 68.72, 69.96, 69.99, 70.59 (each -OCH_2CH_2O-), 114.69 (9-, 10-C), 130.55 (aromatic 2-, 6-C), 132.94 (aromatic 3-, 5-C), 133.24 (4-C), 134.52 (1-C), 134.72 (6-C), 134.81 (aromatic 1-C),138.85 (2-C), 140.32 (5-C), 150.10 (3-C), 161.06 (aromatic 4-C), 162.43 (7-C); m/z 478 (M^+, base peak).

5-(8,8-Dicyanoheptafulven-3-yl)-2-hydroxy-1,3-xylyl-18-crown-5 ***1b***
Anhydrous lithium iodide (0.33 g, 2.5 mmol) and crown ether anisole **4** (0.48 g, 1.0 mmol) were dissolved in dry freshly distilled pyridine (20 cm^{-3}) under argon, and the solution was heated under reflux with stirring for *ca* 6 h.

After cooling to room temperature, pyridine was removed under reduced pressure. The dark brown oily residue was redissolved in 3 $mol \cdot dm^{-3}$ hydrochloric acid (20 cm^{-3}), and then extracted with chloroform, dried, and evaporated to dryness. Column chromatography on deactivated silica gel (SiO_2:water = 100:20) with chloroform–methanol–water (100:1:30, lower phase) as the eluent yielded 5-(8,8-dicyanoheptafulven-3-yl)-2-hydroxy-1,3-xylyl-18-crown-5 **1b**. (recrystallized twice from dichloromethane–ethanol). Yield 76%. Red needles; mp 145–146°C (Found: M^+, 464.2004, $C_{26}H_{28}N_2O_6$ requires M, 464.1947); ν_{max}/cm^{-1} 2209 (C≡N); δ_H ($CDCl_3$) 3.70~3.77 (m, 16H, -OCH_2CH_2O-), 4.71 (s, 4H, benzylic H), 6.98~7.04 (m, 2H, 4- and 5-H), 7.28~7.38 (m, 2H,1- and 6-H), 7.27 (s, 2H, aromatic H), 7.42 (dd, 1H, 2-H), 8.51 (br s, 1H, -OH); δ_C ($CDCl_3$) 69.49 (8-C), 70.06, 70.17, 70.35, 70.71 (each -OCH_2CH_2O-), 115.02, 115.06 (each 9-, 10-C), 125.96 (aromatic 3-, 5-C), 128.54 (aromatic 2-, 6-C), 131.34 (aromatic 1-C), 132.88 (4-C), 134.01 (1-C), 134.66 (6-C), 138.70 (2-C), 140.50 (5-C), 150.74 (3-C), 157.64 (aromatic 4-C), 162.64 (7-C); m/z 464 (M^+, base peak).

Changes in electrical conductivity and UV/Vis absorption spectra

Figure 3(a) shows the specific conductivity of the solution of compound **1b** in DMSO plotted against the molar ratio of lithium hydroxide to compound **1b**. The conductivity of the solution increases linearly from the start of the titration. This represents the neutralization of the weak acid (compound **1b**) and the replacement by its salt. From point A, the conductivity increases with a lower gradient. Point A corresponds exactly to the equivalent of compound **1b**, indicating that the deprotonation reaction proceeded quantitatively.

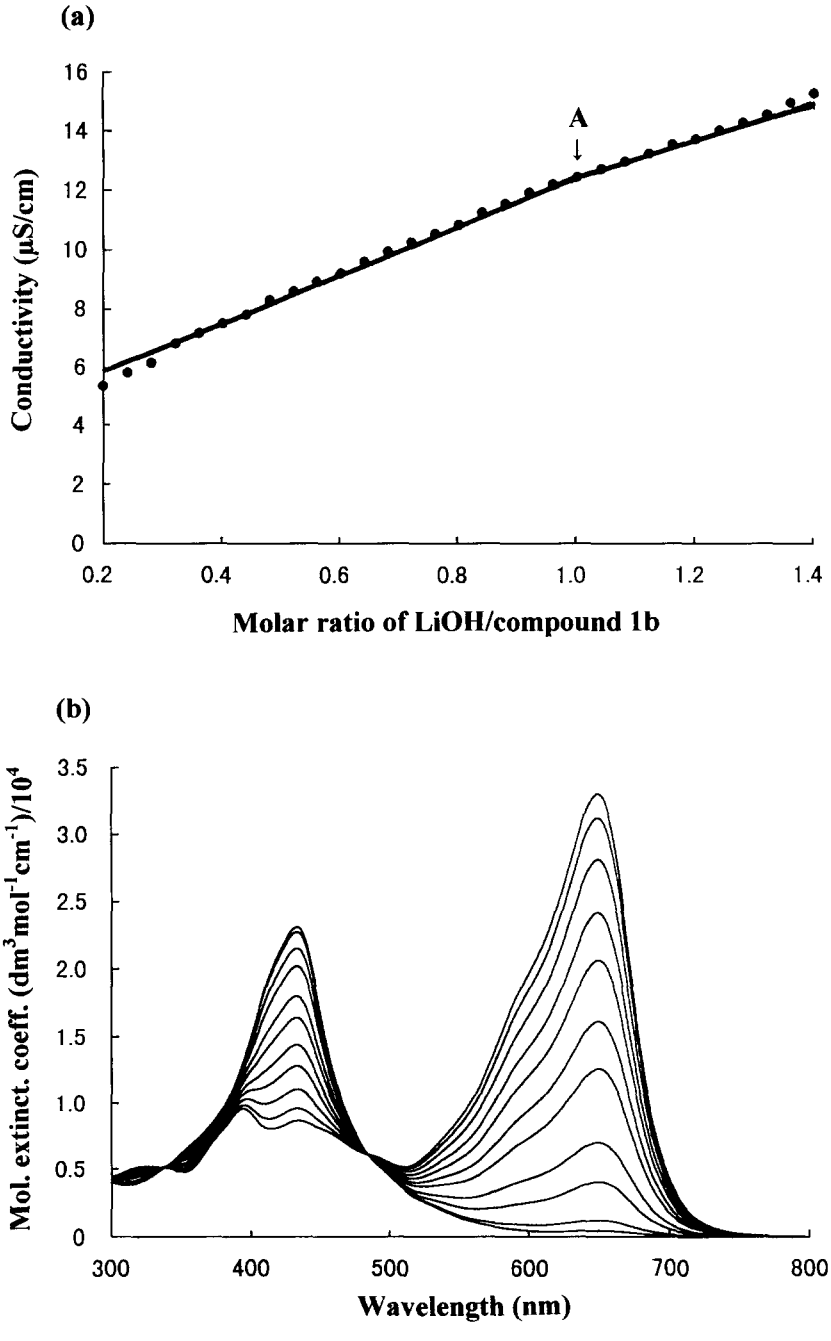

Fig. 3. Changes in electrical conductivity and UV/Vis absorption spectra of compound **1b** in DMSO on deprotonation with LiOH (Li^+: 0.60 Å): (a) conductometric titration and (b) solution spectra.

The absorption spectra of compound **1b** from the initial point to point A are shown in Fig. 3(b). A large spectral shift due to deprotonation is observed from about $\lambda_{max} = 432.0\,nm$ to about $\lambda_{max} = 646.5\,nm$ ($\Delta\lambda_{max} = 214.5\,nm$; $\Delta(\lambda^{-1}) = 7680\,cm^{-1}$). The color of the solution clearly changes from red via green to blue. Two isosbestic points are apparent around $\lambda = 330$ and 480 nm, indicating that the spectral change is based on a binary equilibrium system between the non-deprotonated and deprotonated states. Since the absorption edge at the band around 646.5 nm is so steep and there was no further absorption bands at longer wavelengths, this band is assigned to the 0–0 transition. Consequently, the shoulder around 580 nm can then be attributed to the 0–1 transition.

Figure 4(a) and (b) shows the changes in conductivity in DMSO characterized by a higher gradient from point A and the corresponding absorption spectra on deprotonation with TBAH, respectively. The exact 1:1 deprotonation reaction again proceeded with TBAH, accompanied by the same spectral changes ($\lambda_{max} \approx 644.5\,nm$) as those with LiOH. The results with LiOH and TBAH clearly indicate that the spectral changes are independent of the type and size of the cation added. Deprotonation with other bases [NaOH (Na^+: 0.95 Å), KOH (K^+: 1.33 Å), RbOH (Rb^+: 1.48 Å) and CsOH (Cs^+: 1.69 Å] behaved nearly in the same way as that with LiOH, although the absorption maximum was slightly different for each base: $\lambda_{max} \approx 642.0\,nm$ with NaOH, 628.5 nm with KOH, 635.0 nm with RbOH and 638.0 nm with CsOH. Evidently, the cation-dependent coloration is not operative in the present experiment, in contrast to the proposed mechanism of the metal-selective coloration [6]. It should be also noted that the spectral changes of the crowned compound **1b** are very similar to those of uncrowned compound **1a** (see also Table 2) [2].

Figure 5(a) and (b) shows the changes in conductivity and absorption spectra plotted against the added amount of lithium iodide, respectively. No change in the conductivity gradient or in the absorption spectra are observed. This result indicates that no noticeable interaction takes place between compound **1b** and lithium iodide. The same result was also obtained for other alkali metal iodides such as NaI, KI, RbI and CsI.

Deprotonation experiments in other solvents

Since DMSO (dielectric constant:$\varepsilon = 48.9$) is known as an extremely good cation solvator, further deprotonation experiments were carried out with less polar solvents such as acetonitrile ($\varepsilon = 37.5$), ethanol ($\varepsilon = 25.0$) and THF ($\varepsilon = 8.2$). The summary of changes in the electrical conductivity of the solution, as well as UV/Vis-spectra data, is given in Table 1. Also given is the electrical conductivity of the solution in the presence of a base required for

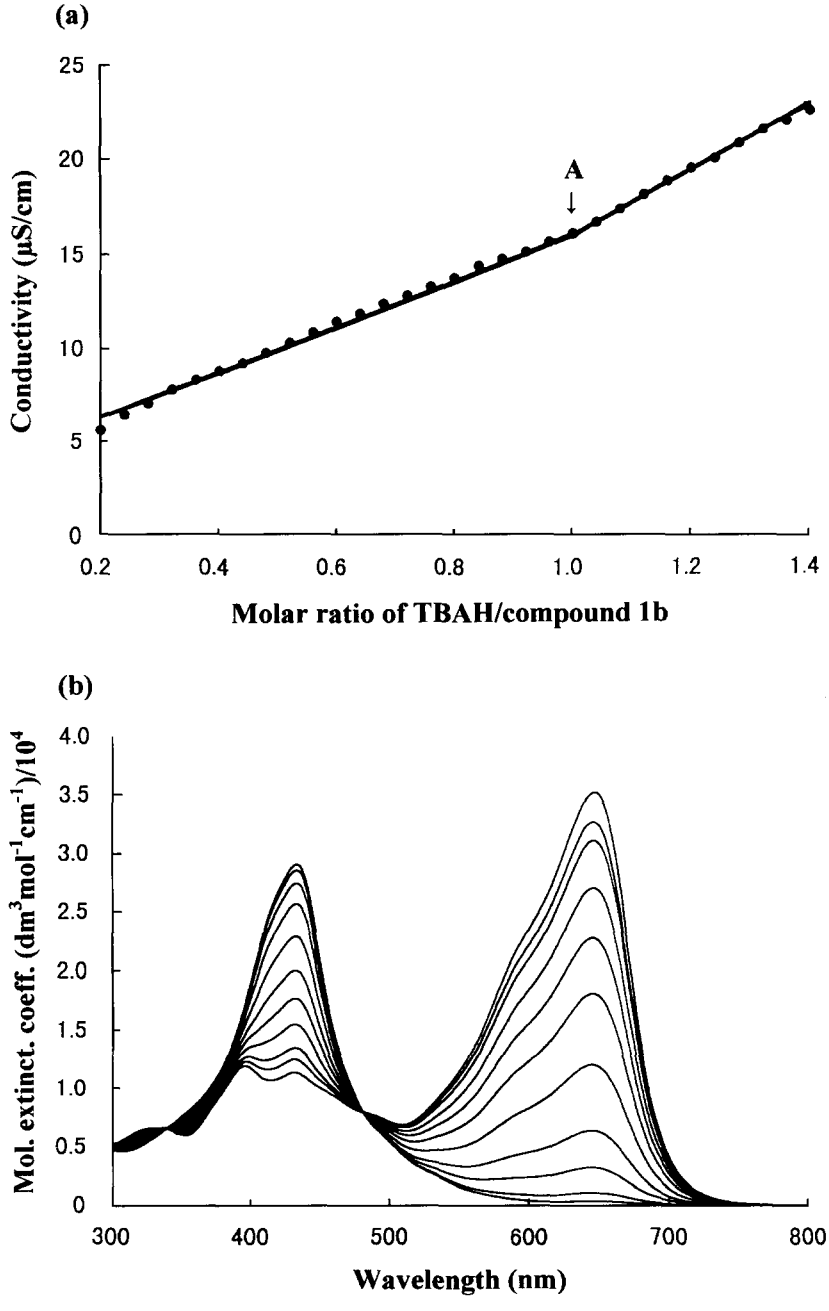

Fig. 4. Changes in electrical conductivity and UV/Vis absorption spectra of compound **1b** in DMSO on deprotonation with TBAH ([n-butyl]$_4$N$^+$OH$^-$): (a) conductometric titration and (b) solution spectra.

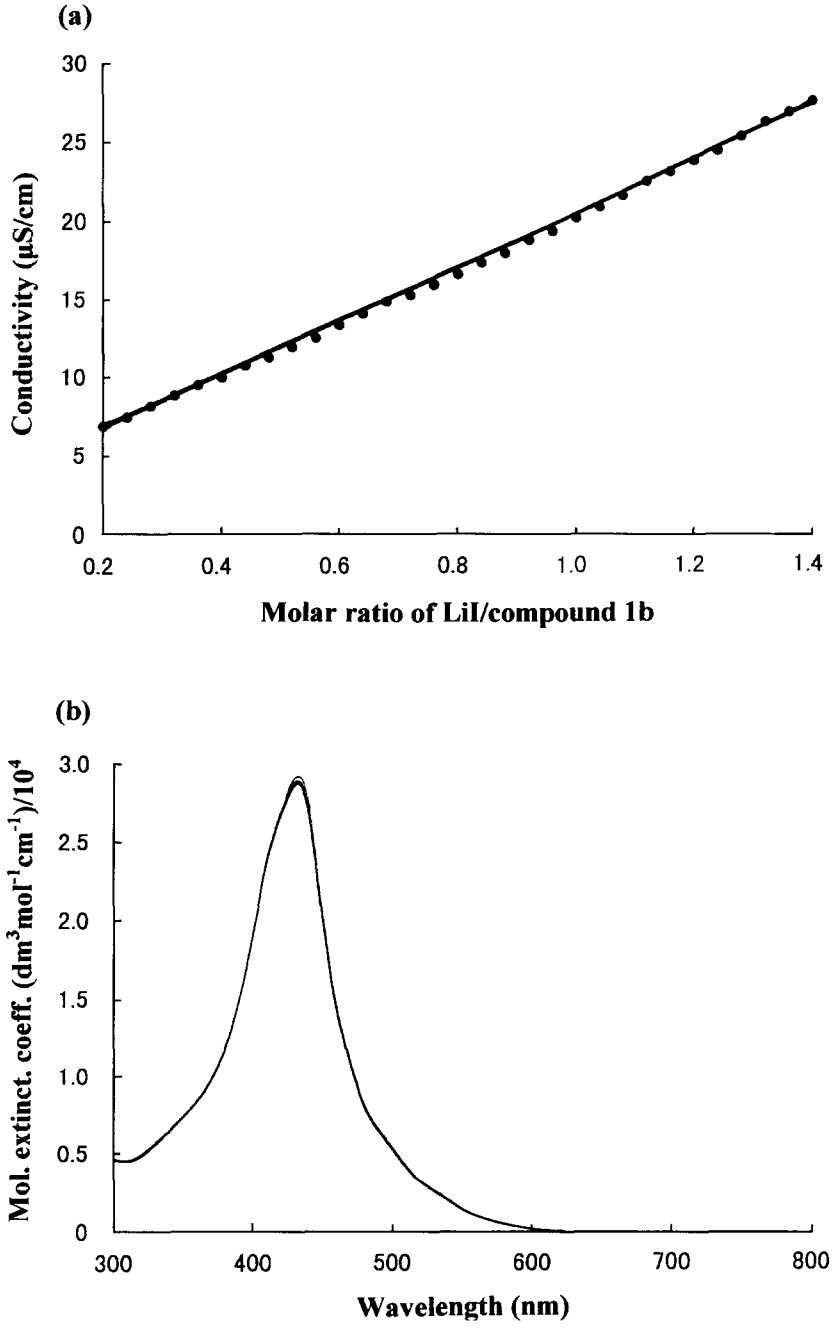

Fig. 5. Changes in electrical conductivity and UV/Vis absorption spectra of compound **1b** in DMSO on addition of LiI: (a) conductometric titration and (b) solution spectra.

TABLE 1
Summary of the Changes in Electrical Conductivity[a] and UV/Vis-spectra

		DMSO ($\varepsilon = 48.9$)	*Acetonitrile* ($\varepsilon = 37.5$)	*Ethanol* ($\varepsilon = 25.0$)	*THF* ($\varepsilon = 8.2$)
LiOH	Electrical conductivity (μS/cm)	~11	~1	~16	~0.06
(Li^+: 0.60 Å)	Conductometric titration	1:1 deprotonation 0–0 transition	Low conductivity, no end-point No significant change	No end-point No significant change	Low conductivity, no end-point No significant change
	UV/Vis-spectra				
NaOH	Electrical conductivity (μS/cm)	~13	~2	~17	~0.06
(Na^+: 0.95 Å)	Conductometric titration	1:1 deprotonation 0–0 transition	1:1 deprotonation 0–1 transition	No end-point No significant change	Low conductivity, no end-point No significant change
	UV/Vis-spectra				
KOH	Electrical conductivity (μS/cm)	~13	~6	~20	~0.02
(K^+: 1.33 Å)	Conductometric titration	1:1 deprotonation 0–0 transition	1:1 deprotonation 0–1 transition	1:1 deprotonation 0–0 ≈ 0–1 transition	Low conductivity, no end-point No significant change
	UV/Vis-spectra				
RbOH	Electrical conductivity (μS/cm)	~14	~9	~18	~0.04
(Rb^+: 1.48 Å)	Conductometric titration	1:1 deprotonation 0–0 transition	1:1 deprotonation 0–1 transition	No end-point No significant change	Low conductivity, no end-point No significant change
	UV/Vis-spectra				
CsOH	Electrical conductivity (μS/cm)	~14	~17	~20	~0.24
(Cs^+: 1.69 Å)	Conductometric titration	1:1 deprotonation 0–0 transition	1:1 deprotonation 0–1 transition	No end-point No significant change	1:1 deprotonation 0–1 transition
	UV/Vis-spectra				
TBAH	Electrical conductivity (μS/cm)	~16	~80	~24	~2.4
	Conductometric titration	1:1 deprotonation 0–0 transition	1:1 deprotonation 0–0 transition	No end-point No significant change	1:1 deprotonation 0–0 transition
	UV/Vis-spectra				

[a]The electrical conductivity of the solution in the presence of a base required for the 1:1 deprotonation reaction but in the absence of compound **1b**.

TABLE 2
Molecular Conformation and UV/Vis Absorption Bands for Compounds **1a** and **1b**

	Heat of formation ($kJ\,mol^{-1}$)	*Dipole moment* (*Debye*)	*Torsion angle* (°)	*Calculated*		*Observed*	
				λ_{max}(*nm*)	f^a	λ_{max}(*nm*)	log ε^b
Compound **1a**							
Initial state	439.3	6.6	45.0	336[c]	0.716	434	4.54
				394[c]	0.338		
Deprotonation state	262.8	3.7	25.3	541[c]	1.246	643	4.60
Compound **1b**:							
Initial state	−516.9	10.4	45–47	364[c]	0.486	431	4.46
				375[c]	0.516		
Deprotonation state	−715.6	8.7	26–29	529[c]	1.120	645	4.55

[a]Oscillator strength.
[b]Molar extinction coefficient.
[c]Major CI components: Compound **1a** (initial): 336 nm: (45→47)/(45→46); 394 nm: (45→46)/(45→47); (deprotonation): 541 nm: HOMO(45)/LUMO(46). Compound **1b** (initial): 364 nm: (89→91)/(89→90); 375 nm: (89→90)/(89→91); (deprotonation): 529 nm: HOMO(89)/LUMO(90), where the number refers to the molecular orbital and the arrow denotes the transition from one orbital to another.

the 1:1 deprotonation reaction but in the absence of compound **1b**. The electrical conductivity serves as a good measure of the solubility of a base in solvents (i.e. degree of dissociation). The λ_{max}-vibronic band is also characterized, for example, by 0–0 or 0–1 transitions. A typical 0–0 transition with λ_{max} can be seen in Figs 3(b) and 4(b); whereas an example of the 0–1 transition with λ_{max} is shown in Fig. 6 (b). The expression 'no significant change' shown in Table 1 implies that only a very small shoulder appears around 650 nm due to deprotonation.

Table 1 clearly indicates that there is a very clear-cut correspondence between the '1:1 deprotonation' reaction and the appearance of the absorption band around 650 nm. Furthermore, another one-to-one correspondence is also recognized between 'no end-point' in conductometric titration and 'no significant change' in UV/Vis-spectra. The result for the 'no end-point' indicates that no deprotonation reaction takes place, resulting in an insignificant change in the UV/Vis-spectra.

In acetonitrile, the 1:1 quantitative deprotonation reaction was observed in all bases except for LiOH. A typical example for CsOH is shown in Fig. 6. The deprotonation reaction was found to proceed very similar to that in DMSO [Figs 3(b) and 4(b)], although the spectral shape in the deprotonated state is slightly different from that for DMSO. The 0–0 transition is the strongest band in the visible region in DMSO, whereas the 0–1 transition becomes the strongest in acetonitrile. The difference in spectral shape is

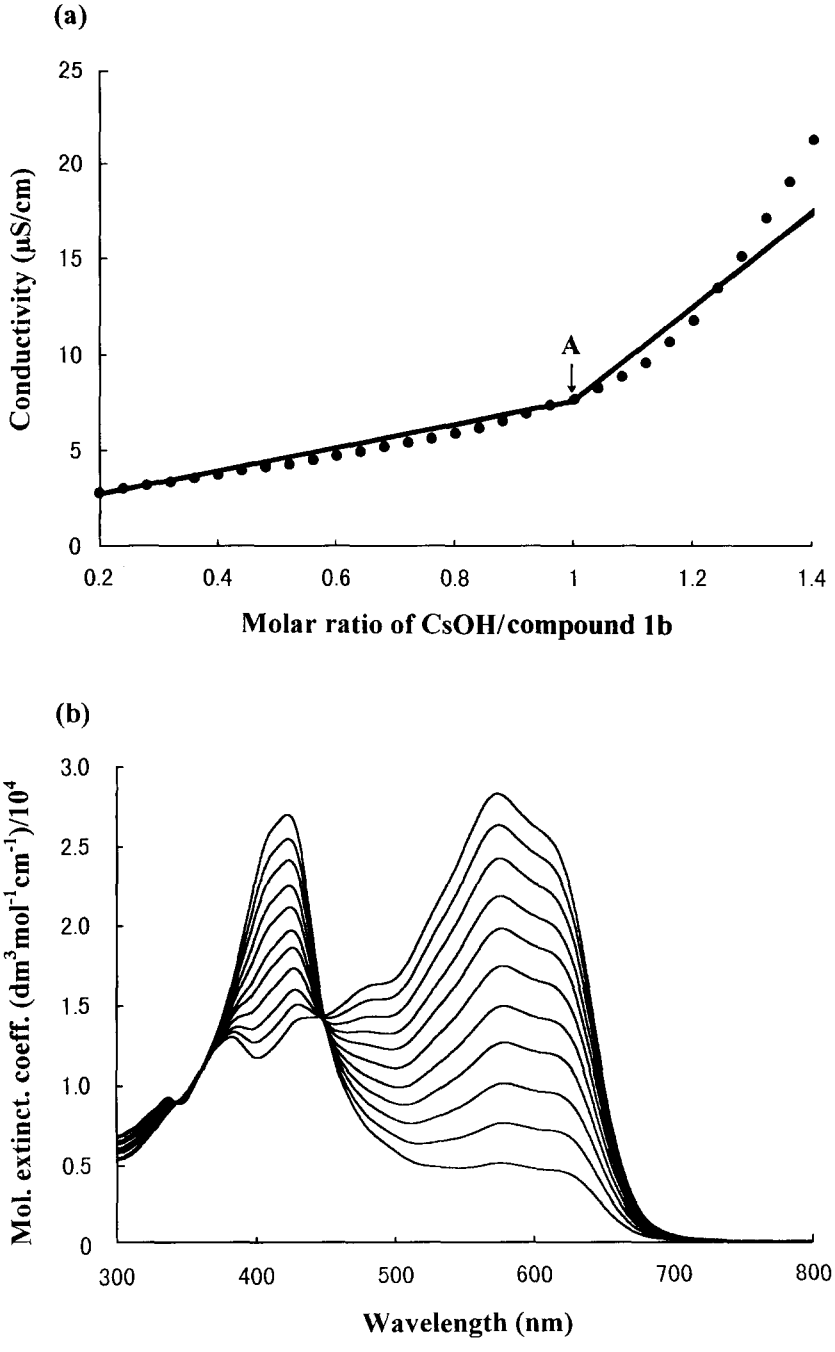

Fig. 6. Changes in electrical conductivity and UV/Vis absorption spectra of compound **1b** in acetonitrile on deprotonation with CsOH: (a) conductometric titration and (b) solution spectra.

ascribed to the molecular surrounding of compound **1b** in each solvent. In the case of LiOH in acetonitrile, no deprotonation is apparent, probably because of the low solubility as shown by the low electrical conductivity of the solution. In contrast, the electrical conductivity of all bases in ethanol is relatively high (i.e. highly soluble). Nevertheless, deprotonation occurs only in KOH. This can be explained in the following way. As is well known, ethanol is a typical amphiprotic solvent which behaves not only as a protic but also as an aprotic solvent. So most of the base added can presumably be used up in the chemical reaction with ethanol, and this explains why deprotonation fails. However, the question why only KOH is effective for deprotonation remains still unanswered.

The solution in THF exhibits, in general, extremely low conductivities compared with those in other solvents. Nevertheless, deprotonation is observed in CsOH and TBAH where the conductivity is higher than in LiOH, NaOH, KOH and RbOH by about one order of magnitude (CsOH) and two orders of magnitude (TBAH). It is also to be noted that deprotonation due to TBAH always gives the 0–0 transition in the UV/Vis-spectra, irrespective of the solvents used.

Geometry optimization and computed spectra

Table 2 illustrates the optimized conformations for the uncrowned compound **1a** [2] and the crowned compound **1b**, together with the computed UV/Vis absorption bands for the initial and deprotonated states. Figure 7(a) and (b) shows the optimized geometry for the initial and deprotonated

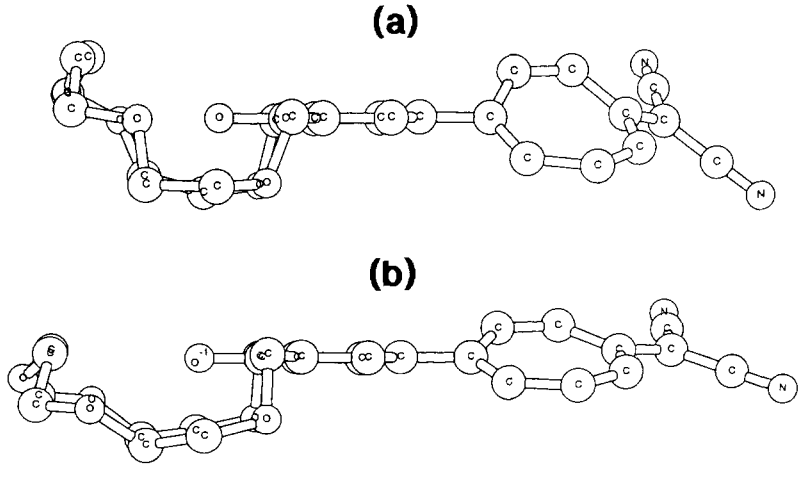

Fig. 7. Optimized geometry for compound **1b** as viewed from the side of the molecule: (a) initial state and (b) deprotonated state. The hydrogen atoms are omitted for clarity.

states of compound **1b** where the hydrogen atoms are omitted for clarity. It is surprising to note that the 18-crown-5 is heavily deformed in such a way that the oxygen atom of the phenolic hydroxide group and those of the crown ether ring repel each other due to electrostatic repulsion of lone pair electrons. In addition, both the seven-membered ring and the phenyl ring are twisted by 45–47° in the initial state. Deprotonation then makes the crown ether ring more wide-opened due to enhanced repulsion caused by the formation of the phenoxide ion ($-O^-$) [Fig. 7(b)]. At the same time, the torsion angle is remarkably reduced to 26–29°, indicating that the π-electrons of the phenoxide part (strong donor) is partly delocalized towards the dicyanomethylene group (strong acceptor), inducing a large bathochromic shift of the UV/Vis absorption band. The tendency of the computed optical absorption bands is in good accord with the experimental observation.

On the other hand, no ring deformation was recognized when only 18-crown-6 (without the hydroxide group in the cavity) was geometry-optimized. The ether ring with a Li^+ in the cavity showed no ring deformation either. This presumably occurs because the electric field inside the cavity is symmetrical about the center in which the metal cation is placed.

The electronic transition in the initial state is composed of two transitions, each of which includes the two major CI-components (CI: configuration interaction): transitions 89→90 (HOMO/LUMO) and 89→91, where the number refers to the molecular orbital. The major transition in the deprotonated state is attributed to the HOMO/LUMO $\pi - \pi*$ transition.

Geometry optimization for crowned compounds **1c** and **1d** revealed that the ring is again heavily deformed in the same fashion as shown in Fig. 7.

Similarities in compounds 1a and 1b on deprotonation

As is evident from Table 2, the conformational and spectral changes of the crowned compound **1b** is very similar to that of the uncrowned compound **1a**, both in experiments and calculations. The present similarity can be explained in the following way. The crown ether ring is considerably deformed out of the plane of the phenyl ring (Fig. 7), so that the phenolic hydroxide is directly exposed to the surroundings. Under these circumstances, the conjugation between the ether ring and compound **1a** is practically blocked and the electronic state of the crowned compound **1b** is approximately equivalent to that of the uncrowned compound **1a**. This explains why no cation-dependent coloration takes place in the present system and why the bathochromic displacement is interpreted as being mainly due to electron delocalization of the phenoxide group ($-O^-$) in the heptafulvene chromophore.

SUMMARY

The UV/Vis spectral changes on deprotonation have been investigated with special attention to the cation-dependent coloration of compound **1b**, using a variety of bases. Deprotonation brought about a drastic color change from red to blue, but quite irrespective of the cation species. Furthermore, the deprotonation behavior is very similar to that of the uncrowned compound **1a**. These facts can be attributed to the heavily deformed crown ether ring due to lone pair repulsion of the oxygen atoms in the cavity. The induced deformation makes the hydroxyl group expose to the surrounding, so that the electronic structure of compound **1b** is nearly equivalent to that of compound **1a**.

A variety of intermediate colors (red via green to blue) appear as the deprotonation reaction proceeds. It should be therefore kept in mind that the metal-selective coloration must be carefully investigated on the firm basis that the deprotonation reaction has been quantitatively completed, otherwise the intermediate color can be misunderstood for a metal-selective coloration.

ACKNOWLEDGEMENTS

The authors express their sincere thanks to Ms L. Chen, K. Ishido and A. Arai for experimental assistance. The authors are also indebted to Mr S. Matsumoto for discussions. The present investigation was partially financed by the CASIO Scientific Foundation.

REFERENCES

1. Brewster, R. Q. and McEwen, W. E., *Organic Chemistry*, 3rd edn. Prentice Hall, Englewood Cliffs, NJ, 1961, p. 486.
2. Otani, H., Sato, Y. and Mizuguchi, J., *Dyes and Pigments*, 1997, **35**, 205.
3. Kaneda, T., Sugihara, K., Kamiya, H. and Misumi, S., *Tetrahedron Letters*, 1981, **22**, 4407.
4. Sugihara, K., Kaneda, T. and Misumi S., *Heterocycles*, 1982, **18**, 57.
5. Reichardt, C., Asharin-Fard, S. and Schäfer, G., *Liebigs Annalen der Chemie*, 1993, 23.
6. Kaneda, T., *Journal of Synthetic Organic Chemistry (Japan)*, 1988, **46**, 96 (in Japanese).
7. Stewart, J. J. P., *MOPAC*, Version 93. Fujitsu.
8. Zerner, M. C., *ZINDO, a General Semi-Empirical Program Package*, 1995, Department of Chemistry, University of Florida, Gainesville, FL.
9. Koenig, K. E., Lein, G. M., Stucker, P., Kaneda, T. and Cram, D. J., *Journal of the American Chemical Society*, 1979, 3553.
10. Oda, M., Funamizu, M. and Kitahara, Y., *Chemistry and Industry (London)*, 1969, **3**, 75.
11. Negishi, E., *Accounts of Chemical Research*, 1982, **15**, 340.